

# Simulink-Based Hardware-in-the-Loop Simulation System for UAV Flight Control System

Shasha Wang<sup>1</sup>, Helong Wu<sup>2,\*</sup>

<sup>1</sup>*School of Information Technology & Engineering, Guangzhou College of Commerce, Guangzhou, China*

<sup>2</sup>*China Electronic Product Reliability and Environment Testing Research Institute Guangzhou, China*

*\*Corresponding Author*

**Abstract:** In the development of flight control systems, hardware-in-the-loop simulation (HIL) simulation is essential for algorithm verification and system validation. By thoroughly and effectively validating flight control algorithms during the ground phase, potential software and hardware issues can be resolved early, significantly reducing losses incurred during actual flight tests. In the event of a crash during real-world flight testing, not only could it cause substantial harm to human life and property, but it would also drastically increase aircraft debugging costs. Currently, HIL are becoming increasingly vital in the development of low-cost, consumer-grade UAV flight control systems, as they greatly enhance development efficiency and debugging safety. This paper proposes a Simulink-based method for constructing an HIL simulation system for UAV flight control. First, the UAV dynamic model is established in the Simulink environment, including the power unit model, control effectiveness model, rigid-body dynamics model, and rigid-body kinematics model. Subsequently, virtual sensor models—such as gyroscopes, accelerometers, magnetometers, and barometers—are developed. Serial communication protocols are employed to facilitate real-time data exchange between the flight control system and the UAV dynamic model, forming a closed-loop HIL simulation. Finally, HIL simulation tests are conducted to evaluate the flight performance of the flight control system. Experimental results demonstrate that the proposed HIL simulation system effectively validates flight control performance, providing robust support for flight control development and testing.

**Keywords:** UAV Body Model; Flight Control; HIL; Virtual Sensor.

## 1. Introduction

At present, HIL simulations are becoming increasingly vital in the development of affordable, consumer-grade UAV flight control systems. These technologies can rapidly improve the efficiency of flight control development and the safety of debugging. Therefore, how to enhance the accuracy of HIL simulations has become a research frontier that scholars at home and abroad are competing to occupy.

The UAV flight control system consists of a sensing system and a controller system. As the front-end of the control system, the sensing system uses multi-sensor data fusion algorithms to calculate the Euler angle information of the UAV's three-axis attitude, which is then output to the control system for control calculation and output. Therefore, HIL simulation of the flight control system requires simulation of both the sensing system and the control system. Existing open-source algorithms for sensing and control systems at home and abroad have shown a diverse and vibrant landscape, with many scholars conducting secondary development based on these open-source algorithms. To verify the effectiveness and rationality of modified algorithms, there is an urgent need to build a UAV flight control HIL simulation test system to conduct HIL simulation tests on flight control performance.

This project focuses on Pixhawk, the world's most popular open-source flight control system, as its research subject. Using model-based design methodology, it establishes a HIL simulation system framework for the sensing and control systems

of UAV flight control. This framework can help researchers accelerate the secondary development of flight control algorithms, reduce development costs, and improve research safety. Additionally, this simulation framework can be applied to education and training, cultivating a large number of UAV flight control development talents for China and promoting the sustainable and stable development of the UAV industry.

## 2. Construction of Flight Control System HIL Simulation System Based on Simulink

### 2.1 Overall Scheme

The design scheme of the UAV flight control system HIL simulation system is shown in Figure 1. The simulation system mainly consists of two parts: the flight control hardware and the Simulink simulation software<sup>[1-3]</sup>. The flight control hardware is connected to the simulation software via a serial port, while the simulation software displays the flight status of the UAV body model in a virtual scenario<sup>[4,5]</sup>. Data interaction between the flight control hardware and the simulation software is realized through a serial port protocol<sup>[6-8]</sup>. Specifically, the

UAV body model outputs sensor data, which is transmitted to the flight control program for calculation to obtain motor PWM speed signals. These PWM speed signals are then sent back to the simulation software to control the UAV body model, forming a closed-loop simulation<sup>[9,10]</sup>. This process enables the UAV flight control system to simulate flight states in real environments, achieving the simulation and testing of flight control performance.

### 2.2 Establishment of UAV Body Model

The UAV body model takes the PWM control signals of motors as input and outputs the state of the multi-rotor and sensor information, simulating a real multi-rotor UAV system. The entire UAV body model comprises four main modules: power unit model, control efficiency model, rigid-body dynamics model, and rigid-body kinematics model. In this project, the Simulink graphical tool is used to construct the aircraft body model, and using the RTW (Real-Time Workshop) toolchain, embedded code is automatically generated for the simulation environment and then flashed to the model debugging system for operational testing. The Simulink models of each module are shown in Figures 1 to 4.

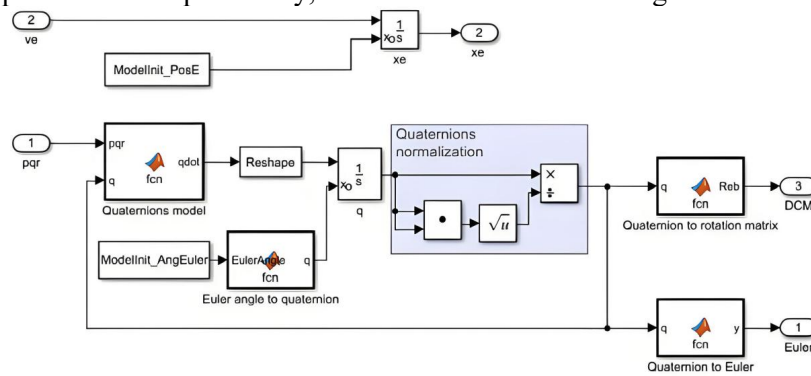


Figure 1. Rigid-Body Motion Model of UAV

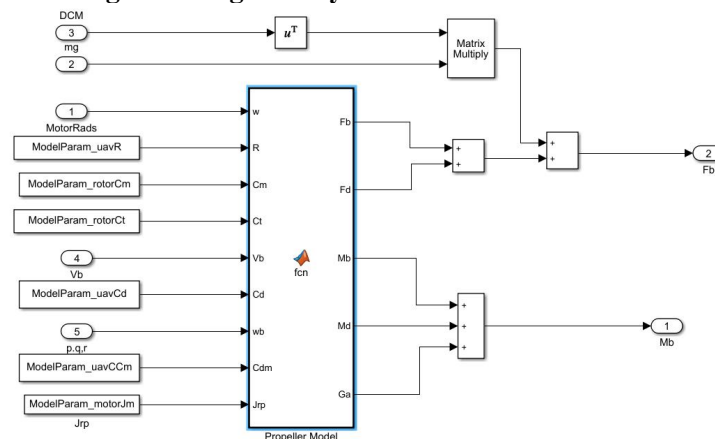


Figure 2. Control Efficiency Model

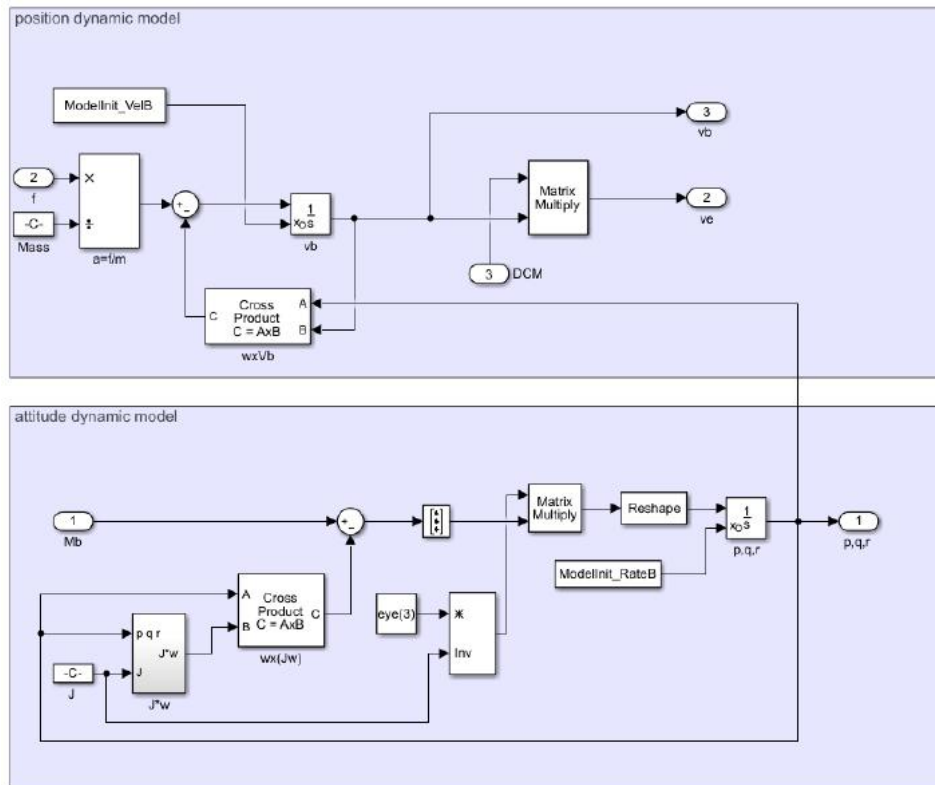


Figure 3. Rigid-Body Dynamics Model

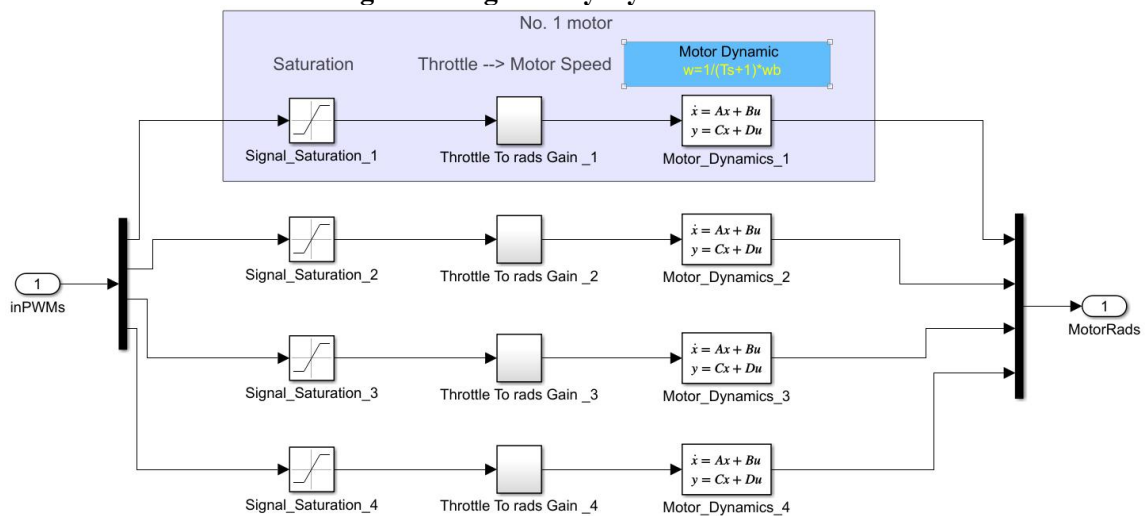


Figure 4. Power Unit Model

The above models are encapsulated into sub-modules, and Figure 5 illustrates the interconnection scheme between the rigid-body control module, power unit module, and control efficiency module. The quadrotor body model takes the PWM control signals of the motors as input and outputs the quadrotor's state and sensor information. It is primarily composed of the power unit model, control efficiency model, and rigid-body control model. The power unit model consists of a power mechanism comprising brushless motors, electronic speed controllers, and

propellers. It takes PWM signals as input and outputs propeller rotational speeds. The control efficiency model calculates the thrust and counter-torque generated by propeller rotation. The rigid-body control model includes both the dynamics model and kinematics model: The dynamics model guarantees that the computed thrust vector remains aligned with the negative Z-axis of the body frame. The kinematic equations derive the complete motion state vector comprising spatial position, velocity, orientation, and rotation rates.

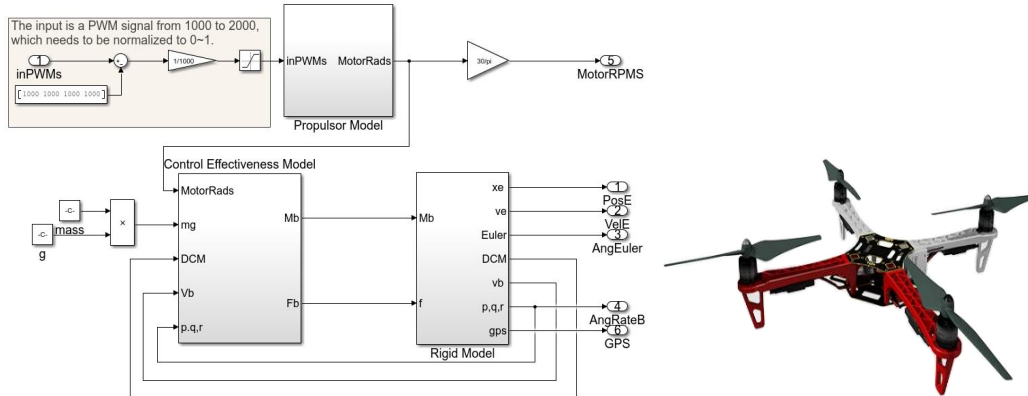


Figure 5. Quadrotor UAV Airframe Model

### 2.3 Establishment of Virtual Sensor Models for Flight Control

The sensor data required for flight control operations is sourced from gyroscopes, accelerometers, magnetometers, barometers, and GPS. As outlined in Section 2, the output values of the quadrotor airframe model only provide gyroscope data AngRateB (angular velocities along the xyz axes) and GPS data PosE (latitude, longitude, and altitude). Data for the accelerometer, magnetometer, and barometer must be reconstructed based on the model's output values. Accelerometer : Measures acceleration values. In the North-East-Down (NED) coordinate system,

$$\begin{bmatrix} a_x \\ a_y \\ a_z \end{bmatrix} = \begin{bmatrix} \cos \varphi \cos \theta & \cos \varphi \sin \theta \sin \varphi - \cos \theta \sin \varphi & \sin \theta \sin \varphi + \cos \theta \cos \varphi \sin \theta \\ \cos \theta \sin \varphi & \cos \theta \cos \varphi + \sin \theta \sin \varphi \sin \theta & \cos \theta \sin \varphi \sin \theta - \cos \varphi \sin \theta \\ -\sin \theta & \cos \theta \sin \theta & \cos \theta \cos \theta \end{bmatrix} * \begin{bmatrix} 0 \\ 0 \\ -g \end{bmatrix} \quad (1)$$

where  $\theta$  is the pitch angle,  $\varphi$  is the roll angle, and  $\psi$  is the yaw angle. The accelerometer model is shown in Figure 6.

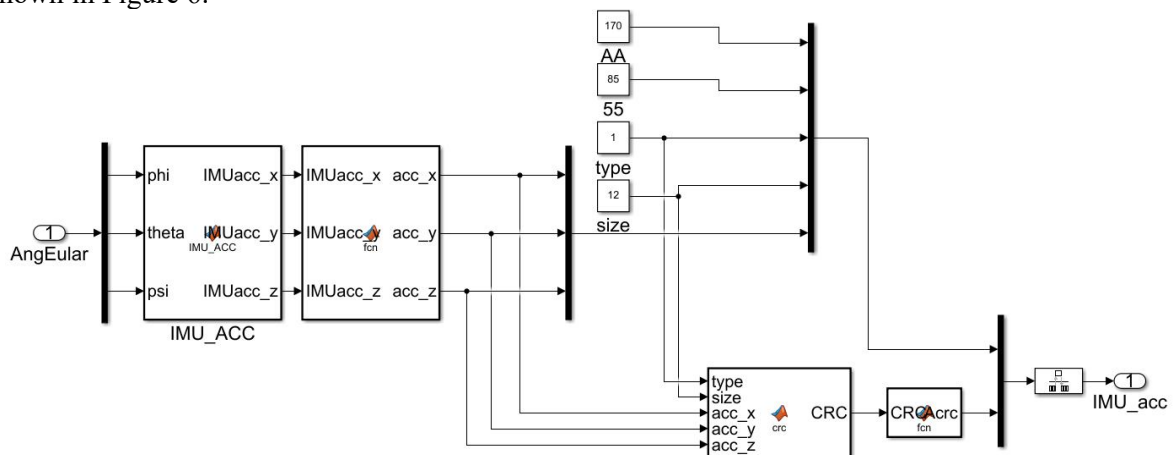


Figure 6. Accelerometer Model

The triaxial magnetometer detects and measures the Earth's magnetic field vector in the UAV's immediate vicinity. When the UAV is stationary with its X-axis facing north, the X-axis aligns with the north direction. In this case, magnetic field strength is only measured

when the accelerometer is placed horizontally with its Z-axis pointing vertically upward, it measures the gravitational acceleration value  $-g$  along the Z-axis, while the X and Y axes read 0, denoted as  $(0, 0, -g)$ . During UAV attitude maneuvers, gravitational acceleration projects vector components onto all three axes of the onboard accelerometer. This process involves transforming the vector  $(0, 0, -g)$  from the earth-fixed coordinate system to the UAV body coordinate system. The relationship between the UAV body frame and the earth frame is defined by a rotation matrix. The triaxial accelerometer values in the UAV body frame are calculated as follows:

along the X-axis, with zero values on the Y and Z axes. Assuming the magnetic field strength is  $B$ , the magnetometer outputs a vector measurement of  $(B, 0, 0)$  in its body-fixed coordinate frame. UAV attitude changes induce rotational transformations of

the magnetic field vector, producing measurable components along each magnetometer axis, which essentially involves transforming the vector  $(B, 0, 0)$  from the earth-fixed coordinate system to the UAV

$$\begin{bmatrix} M_x \\ M_y \\ M_z \end{bmatrix} = \begin{bmatrix} \cos \varphi \cos \theta & \cos \varphi \sin \theta \sin \varphi - \cos \theta \sin \varphi & \sin \theta \sin \varphi + \cos \theta \cos \varphi \sin \theta \\ \cos \theta \sin \varphi & \cos \theta \cos \varphi + \sin \theta \sin \varphi \sin \theta & \cos \theta \sin \varphi \sin \theta - \cos \varphi \sin \theta \\ -\sin \theta & \cos \theta \sin \theta & \cos \theta \cos \theta \end{bmatrix} * \begin{bmatrix} 0 \\ 0 \\ B \end{bmatrix} \quad (2)$$

The triaxial magnetometer model is shown in Figure 7:

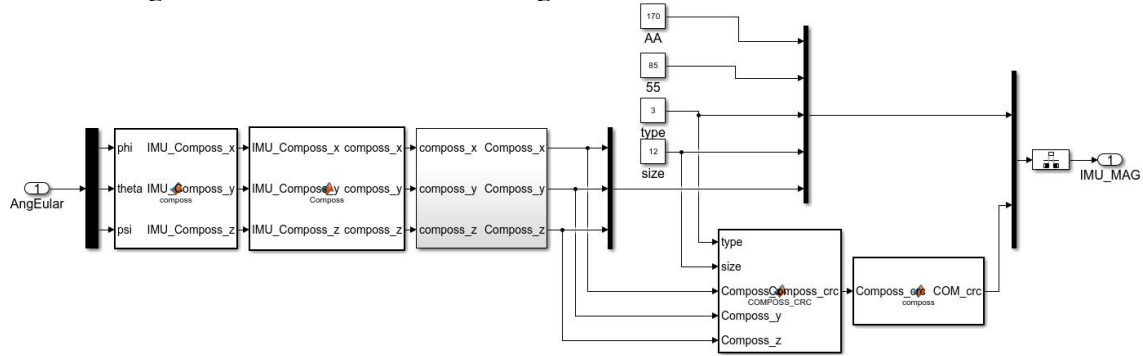


**Figure 7. Triaxial Magnetometer Model**

The barometer is used to measure the altitude of the UAV. In Ardupilot, the barometer altitude is primarily referenced rather than the GPS altitude. The barometric altitude measurement method involves measuring the air pressure  $P_0$  and ground temperature  $T$  at the takeoff point before takeoff, then measuring the air pressure  $P$  at the current altitude during flight. By substituting  $P_0$ ,  $P$ , and  $T$  into the barometric altitude formula, the altitude  $h$  relative to the takeoff point is calculated. In the official Ardupilot code, the following formula is used to calculate the altitude:

$$h = 153.8462T \left\{ 1 - e^{\left[ 0.190259 \lg \left( \frac{P}{P_0} \right) \right]} \right\} \quad (3)$$

When reconstructing barometric pressure data, the inverse transformation of the above formula yields the altitude-to-pressure conversion relationship:

$$P = P_0 \times 10^{\left[ 5.256 \ln \left( 1 - \frac{h}{153.8462T} \right) \right]} \quad (4)$$

### 3. Construction of Hardware-in-the-Loop Simulation System for UAV Flight Control Performance

The HIL simulation setup for UAV flight control system verification appears in Figure 8, consisting of a flight control system, remote controller, Simulink simulation software, FlightGear 3D visual simulation software, and a flight control ground station. The UAV body model runs in Simulink, with the flight control system connected to the simulation software

body coordinate system. The relationship between the UAV body frame and the earth frame is defined by a direction cosine matrix (DCM). The triaxial magnetometer values in the UAV body frame are calculated as:

via a serial port protocol for real-time communication with the UAV body model. The ground control station establishes a data link with the flight control system to provide real-time monitoring of flight parameters throughout the simulation, while FlightGear is used to visually display the UAV's flight status in real time, intuitively showcasing the flight process of the UAV model. The test items that the HIL simulation system can complete are listed in Table 1.

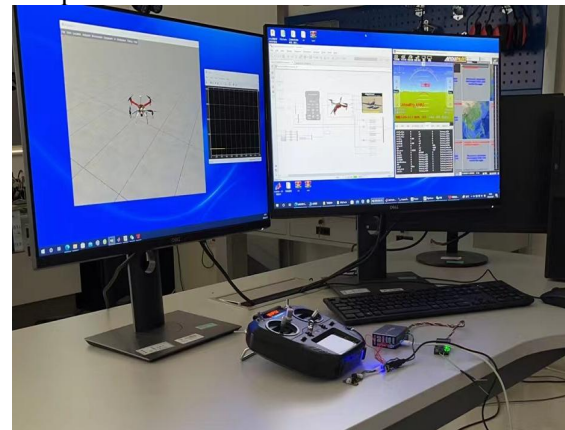


**Figure 8. UAV Flight Control HIL System**

The UAV flight control system's HIL test setup is illustrated in Figure 9. In manual flight mode, the flight control system is operated via a remote controller to command the UAV body model to perform tasks such as takeoff, hover, and landing. During flight, the UAV's movement in forward, backward, left, and right directions is verified to test the control performance of roll, pitch, and yaw.



The experimental results show that the UAV body model correctly responds to remote control commands, demonstrating the effectiveness of the simulation system.

**Table 1. Main Technical Parameters of the Simulated Flight Control System**

No.	Test Type	Test Item Name	Test Item Description
1	Functional Performance	Routine Maneuvers	Includes attitude control and position control.
2		Remote Control	Takeoff, cruise, and landing.
3		Autonomous Cruise	Verify if the UAV can fly normally according to the pre-programmed mission.
4		Mode Switching	Manual mode, self-stabilization mode, altitude hold mode, and position hold mode.



**Figure 9. HIL Simulation Test of UAV Flight Control**

#### 4. Conclusion

This project has completed the development of a Simulink-based HIL simulation system for flight control system. 1. UAV Body Model Establishment: A UAV body model was first created to evaluate the flight control performance by analyzing its flight states. 2. Virtual Sensor Model Construction: Virtual sensor models for gyroscopes, accelerometers, magnetometers, etc., were developed to enable data interaction between the real flight control system and the simulation system, and to verify the safety of the flight control system under abnormal operating conditions. 3. HIL Simulation System Construction: Finally, a Simulink-based HIL simulation system for flight control was built, and HIL simulation tests on flight control performance were conducted. Experimental results show that the HIL simulation system constructed in this thesis can effectively test the flight control performance, providing a laboratory verification method for flight control algorithm testing.

#### Acknowledgments

The authors are supported by the Approved Project of Guangdong Higher Education

Association's 14th Five-Year Plan 2024 Higher Education Research Project (Project No.24GYB75), 2024 Research Project of Guangdong Association of Higher Education Teaching Management (No.GDZLGL2428), the AI+Data Acquisition Technology" Pilot Course of Guangzhou College of Commerce (No.2024rgznsdkc06), "Data Acquisition Technology Course Teaching-Research Office" - 2024 Quality Engineering Project of Guangzhou College of Commerce (No.2024ZLGC11), Higher Education Teaching Reform Project: "Project-Driven and Engineering Practice-Based Teaching Reform and Research for the 'Digital Image Processing' Course"(No. 2024JXGG42), the Development fund for the Fifth Electronics Research Institute of Ministry of Industry and Information Technology under No.23Z07, the Development fund for the Fifth Electronics Research Institute of Ministry of Industry and Information Technology under No.24Z05, the Special Fund of Guangdong Province for promoting high-quality economic development under No.JQR246205070.

#### References

- [1] Sarcinelli-Filho, Mario, Brandao, et al. A Hardware-in-the-Loop Platform for

- Rotary-Wing Unmanned Aerial Vehicles. *Journal of Intelligent & Robotic Systems: Theory & Application*, 2016, 84(1/4):725-743.
- [2] Nguyen K D, Ha C. Development of Hardware-in-the-Loop Simulation Based on Gazebo and Pixhawk for Unmanned Aerial Vehicles. *International Journal of Aeronautical and Space Sciences* 19, 2018: 238–249.
- [3] De C, Dos S. A Software-in-the-Loop Simulation Scheme for Position Formation Flight of Multicopters. *Journal of Aerospace Technology and Management*, 2016, 8(4):431-440.
- [4] Prabowo Y A , Trilaksono B R , Triputra F R . Hardware In-the-Loop Simulation for Visual Servoing of Fixed Wing UAV// 2015 International Conference on Electrical Engineering and Informatics. IEEE, 2015.
- [5] Sung G M, Tung L F, Wang H K, et al. USB Transceiver with a Serial Interface Engine and FIFO Queue for efficient FPGA-to-FPGA Communication. *IEEE Access*, 2020, PP(99):1-1.
- [6] Yang J, Wang X, Baldi S, et al. A software-in-the-loop implementation of adaptive formation control for fixed-wing UAVs. *IEEE/CAA Journal of Automatica Sinica*, 2019, 6(5).
- [7] Ebeid E, Skriver M, Terkildsen K H, et al. A Survey of Open-Source UAV Flight Controllers and Flight Simulators. *Microprocessors and Microsystems*, 2018, 61.
- [8] P Castillo-García, Hernandez L E M , Gil P G . Data Fusion for UAV Localization - ScienceDirect. *Indoor Navigation Strategies for Aerial Autonomous Systems*, 2017:109-129.
- [9] Nak Y K, Wonkeun Y, In H C, et al. Features of Invariant Extended Kalman Filter Applied to Unmanned Aerial Vehicle Navigation. *Sensors*, 2018, 18(9):2855.
- [10] Rabbou M A, El-Rabbany A. Tightly coupled integration of GPS precise point positioning and MEMS-based inertial systems. *GPS Solutions*, 2015, 19(4):601-609.